JMEPEG (2016) 25:2074–2083
DOI: 10.1007/s11665-016-2028-1

1059-9495/$19.00

Effect of Hybrid Surface Modifications on Tensile Properties of Polyacrylonitrile- and Pitch-Based Carbon Fibers

Kimiyoshi Naito

(Submitted November 27, 2015; in revised form February 15, 2016; published online March 31, 2016)

Recent interest has emerged in techniques that modify the surfaces of carbon fibers, such as carbon nanotube (CNT) grafting or polymer coating. Hybridization of these surface modifications has the potential to generate highly tunable, high-performance materials. In this study, the mechanical properties of surface-modified polyacrylonitrile (PAN)-based and pitch-based carbon fibers were investigated. Single-filament tensile tests were performed for fibers modified by CNT grafting, dipped polyimide coating, high-temperature vapor deposition polymerized polyimide coating, grafting-dipping hybridization, and grafting-vapor deposition hybridization. The Weibull statistical distributions of the tensile strengths of the surface-modified PAN- and pitch-based carbon fibers were examined. All surface modifications, especially hybrid modifications, improved the tensile strengths and Weibull moduli of the carbon fibers. The results exhibited a linear relationship between the Weibull modulus and average tensile strength on a log-log scale for all surface-modified PAN- and pitch-based carbon fibers.

Keywords carbon fibers, fracture behavior, hybrid surface modifications, tensile properties, Weibull modulus

1. Introduction

Carbon fibers are widely used as reinforcements in composite materials because of their high specific strengths and moduli (Ref 1). The development of carbon fibers has been driven in two directions: high-tensile-strength fibers with fairly high strain-to-failure rates (~2%) and high-modulus fibers with very high stiffnesses and moderate strengths. Today, high-strength polyacrylonitrile (PAN)-based (>6 GPa) and high-modulus pitch-based (>900 GPa) carbon fibers are commercially available. The tensile and flexural properties of several PAN- and pitch-based carbon fibers were characterized by Naito et al. (Ref 2, 3).

The surfaces of carbon fibers affect the fabrication and use of carbon-fiber-reinforced composites (Ref 4). Carbon nanotube (CNT) grafting is a recently developed technique for modifying the surfaces of carbon fibers (Ref 5-7). Naito et al. recently grafted CNT onto PAN- and pitch-based carbon fibers to improve tensile strengths, fracture behaviors, ductility, Weibull moduli, and thermal conductivities of these fibers (Ref 8, 9). The growth of dense CNT networks on carbon fibers may overcome strength-limiting defects and improve the heat resistances of the fibers.

Polymer coating is another technique for modifying the surfaces of carbon fibers. A compliant polymer coating can potentially correct surface defects in a carbon fiber and improve its ability to absorb impact energy. Carbon fibers have been coated with polymers via dip coating (Ref 10, 11), electropolymerization (Ref 12, 13), and deposition processes (Ref 14, 15). High-temperature vapor deposition polymerization (VDP_H) is a promising approach because it forms relatively uniform thin layers on three-dimensional objects and porous materials. Naito et al. recently investigated the effects of compliant polyimide (PI) nanolayer coatings on the tensile properties of PAN- and pitch-based carbon fibers (Ref 16, 17). Using the VDP_H approach, PI nanolayer coatings can be directly deposited onto each filament within fiber bundles; the PI nanolayers improved tensile strengths and Weibull moduli of the PAN- and pitch-based carbon fibers.

Some of these surface modifications are useful; however, their uses are limited to highly specialized applications. Two or more types of surface modifications may be combined to generate hybrid fibers with the properties of both individual modifications. Similar materials engineering has been achieved for bulk hybrid composites (Ref 18-21).

In the present work, tensile tests were conducted on single filaments of high-strength PAN-based and high-modulus pitch-based carbon fibers to realize several surface modifications, including hybridizations. The Weibull statistical distributions were evaluated for these surface-modified fibers.

2. Experimental

2.1 Materials

High-strength PAN-based carbon fibers (T1000GB; Toray Industries, Inc.) and high-modulus pitch-based carbon fibers (K13D; Mitsubishi Plastics, Inc.) were used in this study. The physical properties of the T1000GB and K13D fibers are listed in Table 1. As received, both fibers had been subjected to

Kimiyoshi Naito, Composite Materials Group, Hybrid Materials Unit, National Institute for Materials Science, 1-2-1 Sengen, Tsukuba, Ibaraki 305-0047, Japan. Contact e-mail: naito.kimiyoshi@nims.go.jp.

commercial surface treatments and sizing (epoxy-compatible sizing).

2.1.1 Carbon Nanotube (CNT) Grafting. The as-received carbon fiber bundles were coated in sizing; prior to use, the carbon fiber bundles were heat-treated at 750 °C for 1 h under vacuum to remove their sizings. Then, an $Fe(C_5H_5)_2$ (ferrocene) catalyst was applied to the T1000GB and K13D carbon fiber bundles using thermal chemical vapor deposition in vacuo to grow CNT on the carbon fibers. Experimental details of the CNT synthesis technique can be found elsewhere (Ref 5-7). The growth temperature for CNT deposition was 750 °C for T1000GB and 700 °C for K13D; the growth time was 900 s.*

2.1.2 Polyimide Coating Using a Dipping Process (DIP-PI). The carbon fiber bundles (without the de-sizing treatment) were used as received. Two types of PI coatings were applied to the carbon fibers: a pyromellitic dianhydride/4,4′-oxydianiline (PMDA/ODA; PI_1) and a 3,3′,4,4′-benzophenone tetracarboxylic dianhydride/4,4′-methylenedianiline (BTDA/MDA; Skybond 703, Industrial Summit Technology Co.; PI_2). Polyamic acid (PAA; poly-4,4′-oxydiphenylene pyromellitamic acid) solutions of these blends were applied to the PAN- and pitch-based single carbon fibers using a dipping process (DIP). Both solutions were diluted with additional *N*-methyl-2-pyrrolidone to obtain viscosities <0.01 Pa·s. After coating, they were heated at 300 °C for 1 h (heating rate: 3 °C/min) in order to imidize the PAA.

2.1.3 Polyimide Coating Using a High-Temperature Vapor Deposition Polymerization Process (VDP_H-PI). A thermoset PI, which was synthesized from PMDA/ODA, was selected as the PI coating for VDP_H; the process was carried out using a polymer coating apparatus (ULVAC Corp., Japan). The VDP_H approach allows the formation of a solvent-free thin layer on a complex-topology substrate; details of this approach are described in the literature (Ref 22-24), and experimental details of the PI coating synthesis technique can be found elsewhere (Ref 23, 24). The specimens were prepared by fixing both ends of the carbon fiber bundles onto a metal plate, which aligned the fibers and applied a constant tension. The carbon fiber bundles were set in a VDP_H chamber and heated at 200 °C. The evaporation temperatures of the PMDA and ODA monomers were 190 °C and 188 °C, respectively. The vaporized monomers entered the vacuum chamber, and the PMDA/ODA coating was deposited and synthesized on the bundles in a vacuum with a pressure of $<2\times10^{-2}$ Pa. After coating, the bundles were heated at 300 °C for 1 h (heating rate: 3 °C/min) in order to imidize the PAA.

2.1.4 Hybridization of CNT Grafting and Polyimide Coating Using a Dipping Process (CNT + DIP-PI). CNTs were grafted on the T1000GB and K13D carbon fibers using a procedure similar to that in section 2.1.1. To synthesize a PI coating on the CNT-grafted carbon fibers, a BTDA/MDA PAA solution was applied to the CNT-grafted PAN- and pitch-based single carbon fibers using the DIP procedure, as described in section 2.1.2.

*Several growth temperatures and times were examined for CNT deposition (e.g., 650, 700, 750, and 800 °C and 120, 300, 600, 900, 1200, and 1800 s). SEM micrographs showed that the quality of CNT deposition was similar for PAN- and pitch-based carbon fibers at the above growth conditions. Differences due to temperature were attributed to the differing thermal conductivities and surface morphologies of PAN- and pitch-based carbon fibers.

Table 1 Mechanical and physical properties of PAN- and pitch-based carbon fibers

	PAN-based							Pitch-based					
	T1000GB (T1000GB-12000-40D)							K13D (K13D2U)					
Fiber	As-received[b]	CNT[b]	DIP-PI_1	DIP-PI_2	VDP_H-PI[b]	CNT + DIP-PI_2	CNT + VDP_H-PI	As-received[b]	CNT[b]	VDP_H-PI[b]	CNT + DIP-PI_2	CNT + VDP_H-PI
Density[a], ρ (g/cm^3)	1.80	…	…	…	…	…	…	2.20	…	…	…	…
Diameter, d_f (μm)	5.03 (0.23)	5.05 (0.27)	5.10 (0.15)	5.09 (0.24)	5.20 (0.39)	5.06 (0.20)	5.10 (0.15)	11.72 (0.36)	11.58 (0.51)	11.80 (0.70)	11.76 (0.55)	11.69 (0.58)
Tensile strength, σ_f (GPa)	5.69 (1.02)	6.73 (1.01)	6.27 (1.02)	6.19 (1.01)	6.49 (0.98)	6.90 (0.85)	7.78 (0.77)	3.21 (0.81)	4.09 (0.85)	3.40 (0.82)	4.88 (0.81)	5.41 (0.81)
Tensile modulus, E_f (GPa)	291 (11)	300 (12)	296 (19)	294 (14)	306 (19)	301 (13)	305 (18)	940 (48)	989 (96)	947 (54)	949 (96)	981 (79)
Failure strain, ε_f (%)	2.06 (0.40)	2.26 (0.36)	2.11 (0.24)	2.10 (0.25)	2.12 (0.34)	2.28 (0.18)	2.55 (0.11)	0.36 (0.08)	0.42 (0.09)	0.36 (0.08)	0.51 (0.04)	0.55 (0.04)
Weibull modulus, m_f	5.86	7.15	6.62	6.56	6.98	8.42	10.00	4.23	5.09	4.40	6.43	6.90

[a]Producer's data sheet. T1000GB: Catalog for TORAYCA, Toray Industries, Inc. (Toray), High-performance carbon fiber Torayca in Japanese, 2004. K13D: Catalog for DIALEAD, Mitsubishi Plastics, Inc., High-performance coal tar pitch carbon fiber. 2009
[b]Single-filament tensile data (25 mm gage length, corrected for machine compliance) from previous investigation (Ref 2, 8, 17)
() indicates standard deviations

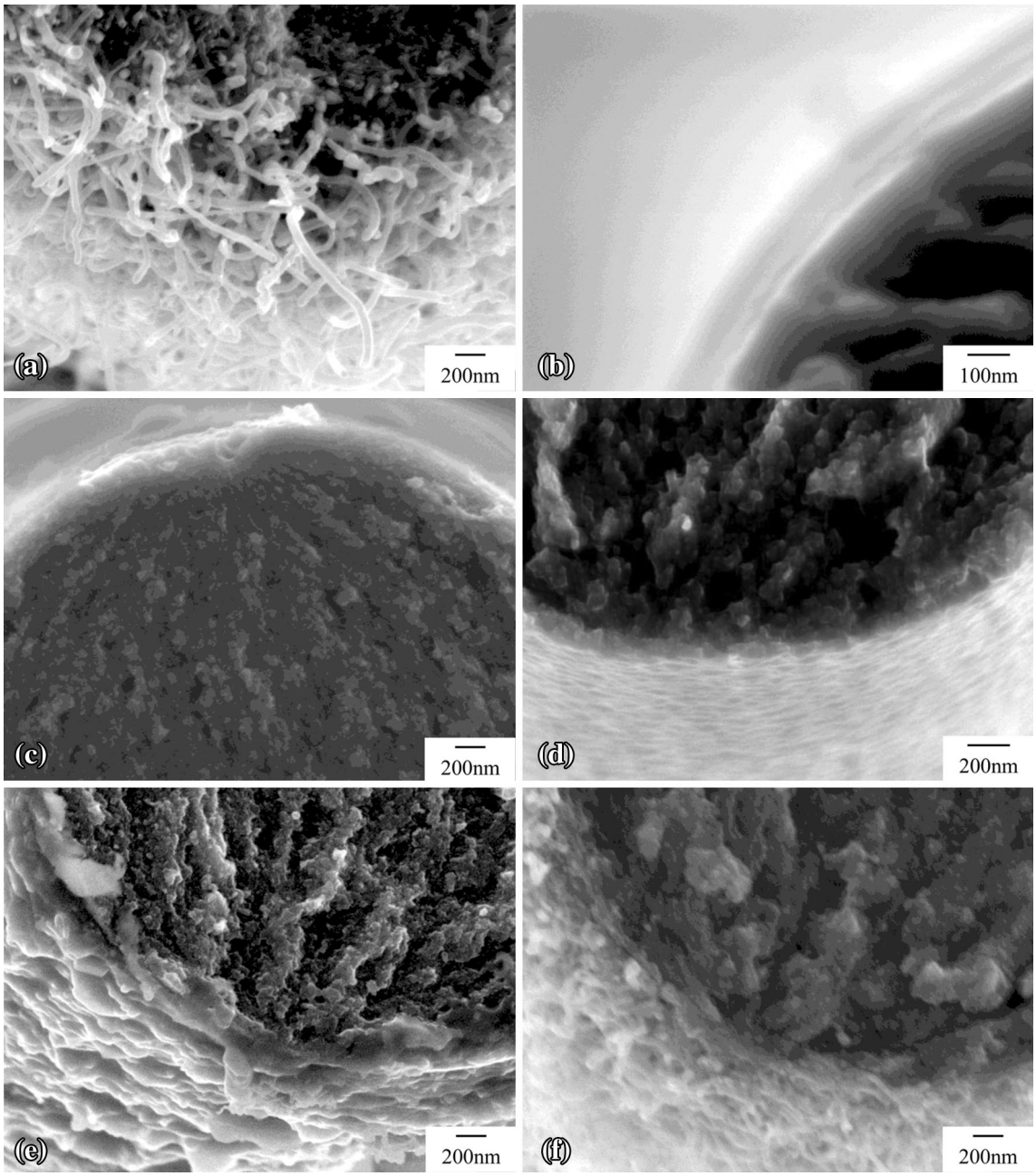

Fig. 1 SEM micrographs of T1000GB (PAN-based) carbon fibers whose surfaces were modified using (a) CNT, (b) DIP-PI_1, (c) DIP-PI_2, (d) VDP_H-PI, (e) CNT + DIP-PI_2, and (f) CNT + VDP_H-PI treatments

2.1.5 Hybridization of CNT Grafting and Polyimide Coating Using a High-Temperature Vapor Deposition Polymerization Process (CNT + VDP_H-PI). CNTs were grafted onto the T1000GB and K13D carbon fibers using a procedure similar to that described in section 2.1.1. To synthesize a PI coating on the CNT-grafted carbon fibers, PMDA/ODA was applied to the CNT-grafted PAN- and pitch-based single carbon fibers using the VDP_H procedure, as described in section 2.1.3.

The surfaces of the modified carbon fibers were examined using a high-resolution scanning electron microscope (SEM; JEOL, JSM-6500F) at an operating voltage of 5 kV. SEM micrographs of CNT, DIP-PI_1, DIP-PI_2, VDP_H-PI, CNT + DIP-PI_2, and CNT + VDP_H-PI modifications are shown in Fig. 1 and 2 for the T1000GB and K13D carbon fibers, respectively. The T1000GB fibers have comparatively smooth surfaces, while the K13D fibers exhibit groove-like features parallel to the fiber axis. The CNT grafting, dipped/polymerized PI coatings, and CNT grafting/PI coating hybridization were successfully performed on both the T1000GB and K13D fibers. CNT could be grafted nearly perpendicular to the fiber surfaces and grown uniformly and densely on the T1000GB and K13D fibers. Individual CNT could be interconnected with each other in several geometries, forming three-dimensional network structures on the fiber surfaces. The outer diameters of the CNT ranged from 30 nm to 50 nm on the T1000GB fibers and from 60 to 80 nm on the

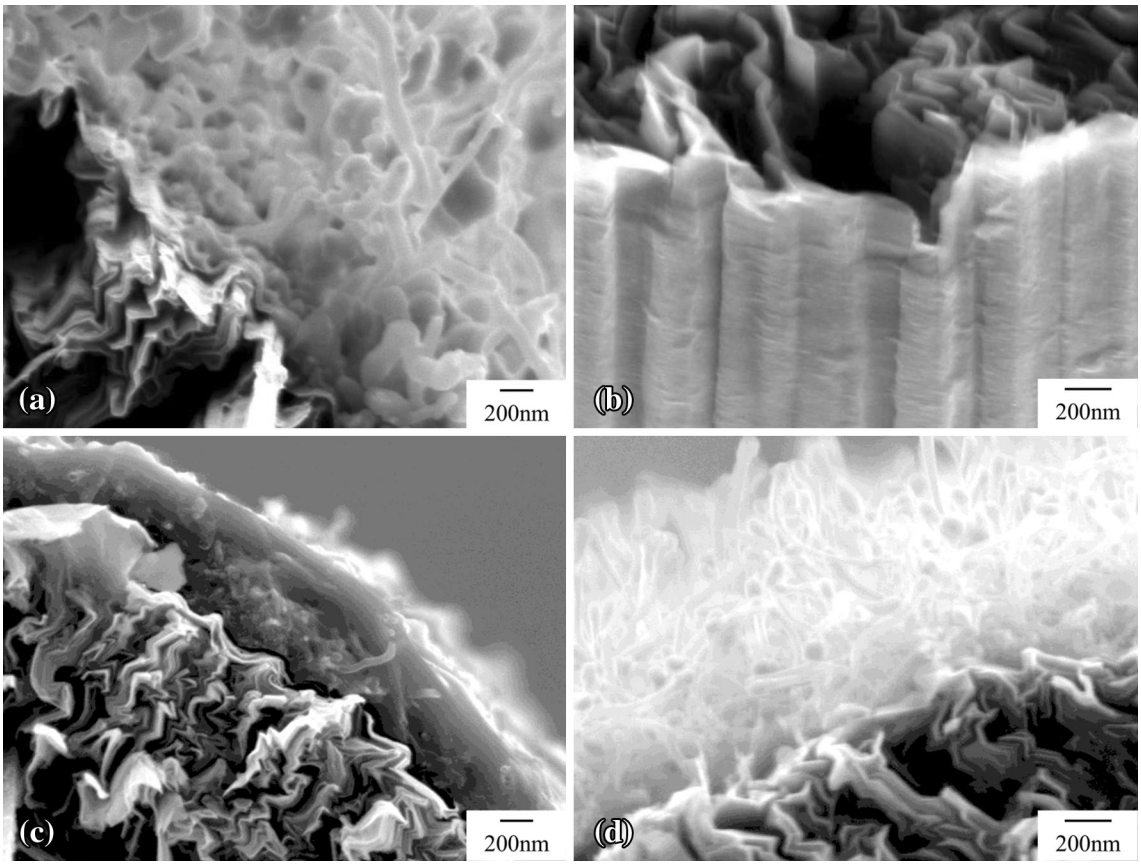

Fig. 2 SEM micrographs of K13D (pitch-based) carbon fibers whose surfaces were modified using (a) CNT, (b) VDP_H-PI, (c) CNT + DIP-PI_2, and (d) CNT + VDP_H-PI treatments

K13D fibers (as shown in Fig. 1(a) and 2(a)). Using the dipping and VDP_H processes, the PI coating was uniformly deposited onto the fiber surfaces. The thickness of the coating on each of the fibers was measured to be ~100 nm (as shown in Fig. 1(b), (c), (d), and 2(b)). For CNT + DIP-PI_2 hybridization, the CNTs were covered with PI coating; the thickness of the coating on the CNT was ~200 nm. The CNTs were not observed because they were coated with PI. However, dimples in the PI coating on CNT were observed for PAN-based carbon fibers, as shown in Fig. 1(e).** A cross-sectional view is shown in Fig. 2(c); CNTs are visible beneath the PI coating. Pitch-based carbon fibers also exhibited dimpling of the PI coating when CNTs were present.† For CNT + VDP_H-PI hybridization, the CNTs were coated with thin PI layers, and the individual CNTs were clearly observed (as shown in Fig. 1(f) and 2(d)).

2.2 Specimen Preparation

Single-filament carbon fiber specimens were prepared on a stage using a stereoscope. A single filament was selected from the carbon fiber bundle and was cut perpendicular to the fiber axis with a razor blade. The diameter of the single carbon fiber d_f was measured from the SEM images. The values of d_f are shown in Table 1 (the average diameters and standard deviations were computed from repeated measurements of each kind of carbon fiber). Before testing, all specimens were stored in a desiccator at 20 ± 3 °C and 10 ± 5% relative humidity.

2.3 Tensile Testing

Tensile tests of single carbon fibers were performed using a universal testing machine (EZ-Test, table top-type tester; Shimadzu) with a 10 N load cell. Each tensile specimen was prepared by fixing the filament onto a paper holder with an instant cyanoacrylate adhesive, as reported elsewhere (Ref 25, 26). Each holder was cut into two parts, and each specimen was placed in the testing machine. The fracture surfaces of the carbon fibers after the single-fiber tensile tests were difficult to observe due to the tiny dimensions of the carbon fibers. Therefore, plastic films were placed on both sides of the carbon fiber filaments and were filled with water to avoid secondary damage to the carbon fibers and to retain the samples. A gage length L of 25 mm was selected, and a crosshead speed of 0.5 mm/min was applied. All tests were conducted in the laboratory environment (23 ± 3 °C and 50 ± 5% relative humidity). Twenty specimens were tested for each type of carbon fiber.

The tensile test measured the load P as a function of extension U up to mechanical failure. Tensile stress σ and tensile strain ε were calculated using

**Similar results are also shown in Fig. 4(e).
†This result is shown in Fig. 5(c).

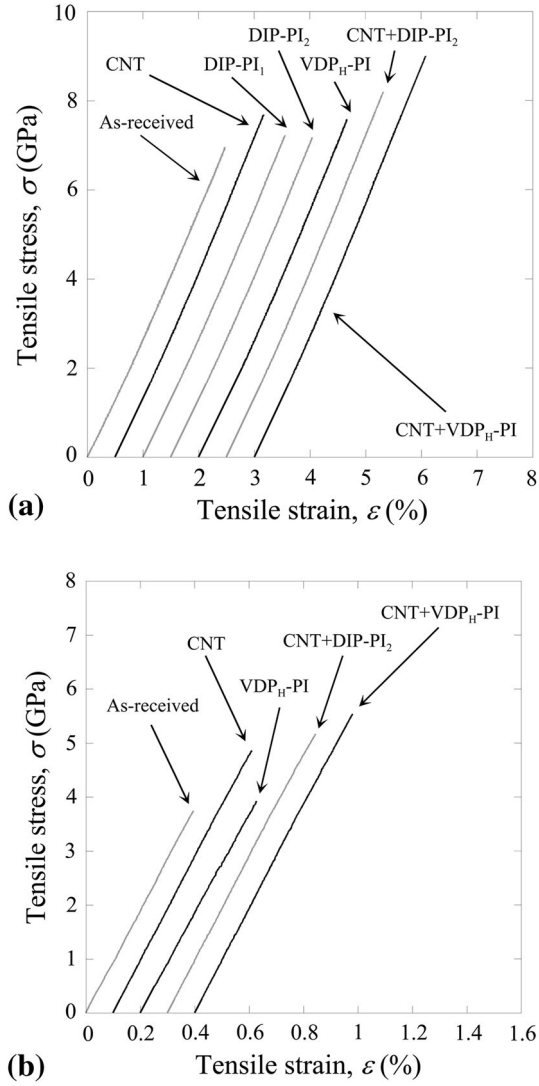

Fig. 3 Typical tensile stress-strain curves for the as-received and surface-modified carbon fibers. (a) T1000GB (PAN-based) carbon fibers and (b) K13D (pitch-based) carbon fibers

$$\sigma = \frac{P}{\left(\frac{\pi d_f^2}{4}\right)} \quad \text{(Eq 1)}$$

and

$$\varepsilon = \frac{U - C_s P}{L}, \quad \text{(Eq 2)}$$

respectively, where C_s is the system compliance and was determined in accordance with ASTM C1557 (Ref 25). The tensile moduli were calculated using a least squares method for the straight-line sections of the stress-strain curves. The fracture morphologies of these carbon fibers were examined using high-resolution SEM.

3. Results and Discussion

3.1 Stress-Strain Relationship

Typical single-fiber tensile stress-strain (σ-ε) curves for CNT, DIP-PI_1, DIP-PI_2, VDP_H-PI, CNT + DIP-PI_2, and CNT + VDP_H-PI modifications are shown in Fig. 3 for T1000GB and K13D carbon fibers. The σ-ε curves for T1000GB and K13D fibers with sizing (in the as-received state) are also shown in this figure. All carbon fibers, with and without surface modification, exhibited linear stress-strain relationships until fracture. The average tensile modulus (E_f), strength (σ_f), and failure strain (ε_f) are summarized in Table 1.

The results show that the tensile moduli of the CNT, DIP-PI_1, DIP-PI_2, VDP_H-PI, CNT + DIP-PI_2, and CNT + VDP_H-PI modifications on PAN- (300 (16) GPa) and pitch-based carbon fibers (967 (83) GPa) are similar to the moduli of the as-received fibers (291 (11) and 940 (48) GPa for T1000GB and K13D, respectively). This result indicates that the tensile moduli of the carbon fibers were unaffected by the surface treatments, such as CNT grafting, PI coating, and hybridization. The tensile moduli of surface-modified carbon fibers exhibit fiber-dominated behaviors in the fiber direction.

The average tensile strengths of T1000GB fibers modified by CNT, DIP-PI_1, DIP-PI_2, VDP_H-PI, CNT + DIP-PI_2, and CNT + VDP_H-PI were determined to be 6.73 (1.01) GPa (Ref 8), 6.27 (1.02) GPa, 6.19 (1.01) GPa, 6.49 (0.98) GPa (Ref 17), 6.90 (0.85) GPa, and 7.78 (0.77) GPa, which are 18, 10, 9, 14, 21, and 37% higher, respectively, than the tensile strength of the as-received fiber (5.69 (1.02) GPa (Ref 2)). The ductility of T1000GB fibers modified by CNT, DIP-PI_1, DIP-PI_2, VDP_H-PI, CNT + DIP-PI_2, and CNT + VDP_H-PI increased relative to that of the as-received fibers.

The average tensile strengths of the K13D fibers modified by CNT, VDP_H-PI, CNT + DIP-PI_2, and CNT + VDP_H-PI were 4.09 (0.85) GPa (Ref 8), 3.40 (0.82) GPa (Ref 17), 4.88 (0.81), and 5.41 (0.81) GPa, which are 27, 6, 52, and 69% higher, respectively, than the tensile strength of the as-received fiber (3.21 (0.81) GPa (Ref 2)). The ductility of the K13D fibers modified by CNT, DIP-PI_1, DIP-PI_2, VDP_H-PI, CNT + DIP-PI_2, and CNT + VDP_H-PI increased relative to that of the as-received fiber.

Surface modifications, especially the hybrid surface modifications, were shown to improve the tensile properties of the PAN- and pitch-based carbon fibers.

3.2 Fracture Morphology

The SEM micrographs shown in Fig. 4 and 5 depict the transverse cross-sectional views of the tensile-fractured surfaces of the surface-modified T1000GB and K13D carbon fibers, respectively. The fracture morphologies of the surface-modified fibers are similar to those of the as-received fibers (Ref 2). Surface defects on the T1000GB carbon fibers were shown to initiate failures; however, the failure initiation sites were obscured on the K13D carbon fibers.

3.3 Weibull Modulus

The results shown in Table 1 clearly indicate that there is appreciable scatter in the tensile strength values. The statistical distribution of fiber tensile strength is usually described by the two-parameter Weibull equation (Ref 27):

$$P_F = 1 - \exp\left[-L\left(\frac{\sigma_f}{\sigma_0}\right)^{m_f}\right], \quad \text{(Eq 3)}$$

where P_F is the cumulative probability of failure of a carbon fiber of length L at applied tensile strength σ_f, m_f is the Weibull modulus (Weibull shape parameter) of the carbon fiber,

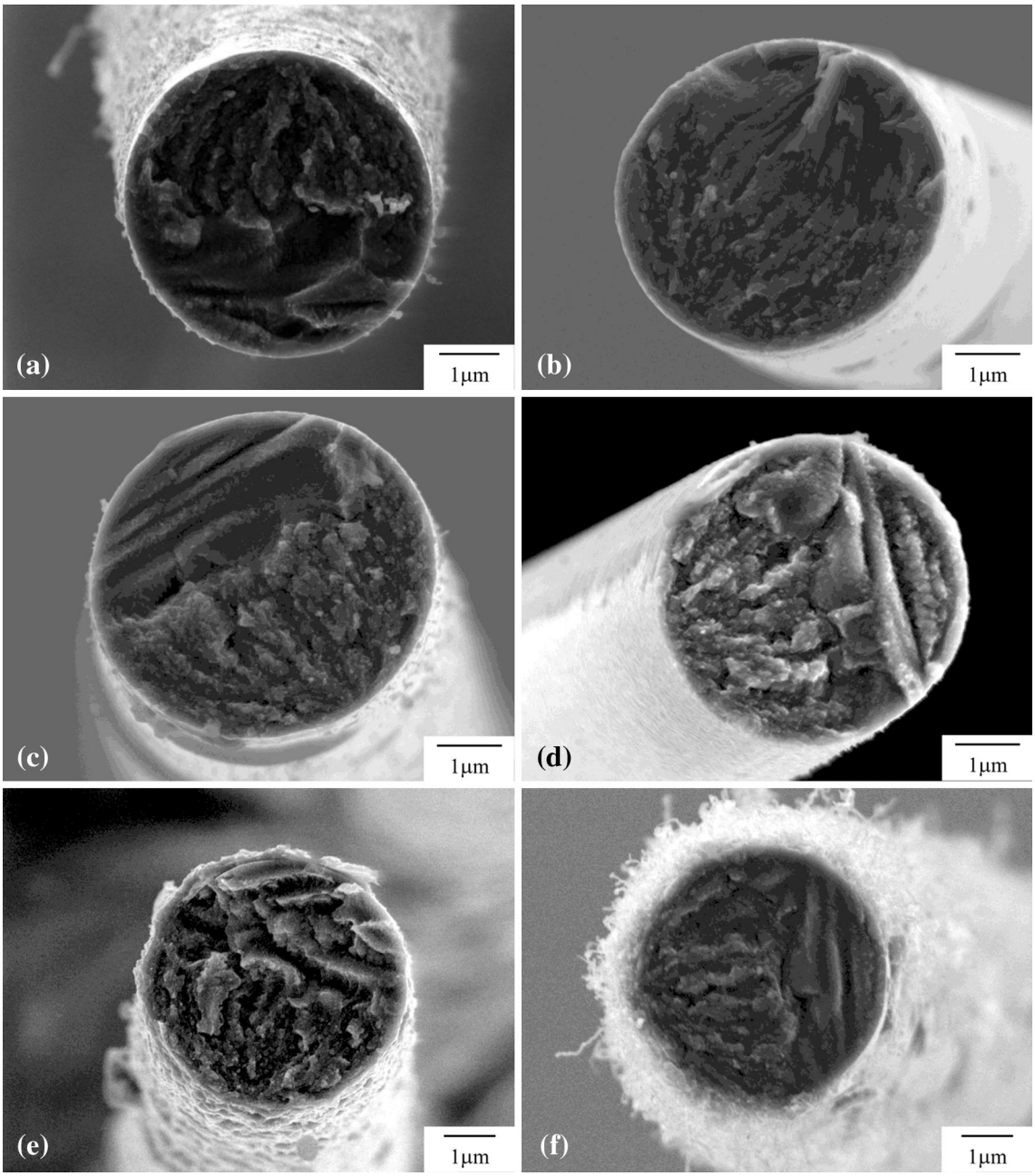

Fig. 4 SEM micrographs of tensile-fractured surfaces showing transverse cross-sectional structures of T1000GB carbon fibers whose surfaces were modified using (a) CNT, (b) DIP-PI_1, (c) DIP-PI_2, (d) VDP_H-PI, (e) CNT + DIP-PI_2, and (f) CNT + VDP_H-PI treatments

and σ_0 is the Weibull scale parameter (characteristic stress). The cumulative probability of failure under a particular stress is given by

$$P_F = \frac{i}{n+1}, \qquad \text{(Eq 4)}$$

where i is the number of fibers that have broken at or below the given stress level and n is the total number of fibers tested. Rearrangement of the two-parameter Weibull expression (Eq 3) gives the following:

$$\ln\left(\ln\left[\frac{1}{1-P_F}\right]\right) = m_f \ln(\sigma_f) - m_f \ln\left(\sigma_0 L^{-\frac{1}{m_f}}\right). \qquad \text{(Eq 5)}$$

Hence the Weibull modulus can be obtained from the linear regression of a Weibull plot based on Eq 5.

Weibull plots of several surface-modified T1000GB and K13D carbon fibers are shown in Fig. 6. The Weibull moduli for T1000GB fibers modified by CNT, DIP-PI_1, DIP-PI_2, VDP_H-PI, CNT + DIP-PI_2, and CNT + VDP_H-PI were calculated to be 7.15 (Ref 8), 6.62, 6.56, 6.98 (Ref 17), 8.42, and

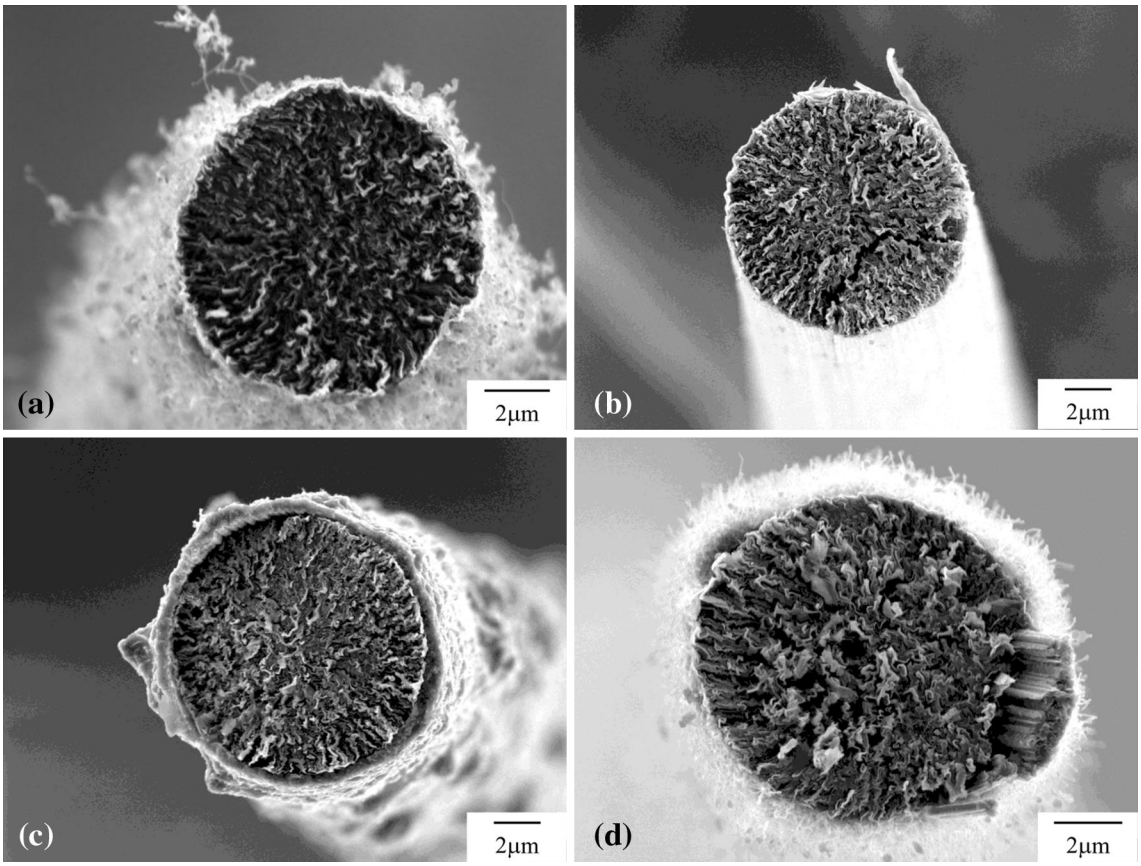

Fig. 5 SEM micrographs of tensile-fractured surfaces showing transverse cross-sectional structures of K13D carbon fibers whose surfaces were modified using (a) CNT, (b) VDP_H-PI, (c) CNT + $DIP\text{-}PI_2$, and (d) CNT + VDP_H-PI treatments

10.00, respectively. The Weibull moduli for K13D fibers modified by CNT, VDP_H-PI, CNT + $DIP\text{-}PI_2$, and CNT + VDP_H-PI were calculated to be 5.09 (Ref 8), 4.40 (Ref 17), 6.43, and 6.90, respectively. The Weibull moduli for the T1000GB and K13D fibers with sizing (in the as-received state) were found to be 5.86 and 4.23, respectively (Ref 2).

The results clearly show that all surface modifications, particularly the hybrid modifications, improved the Weibull moduli of the T1000GB and K13D carbon fibers.

The Weibull modulus differences can be attributed to the natures and distributions of flaws in the fibers. It is well known that many defects in carbon fibers, including fibrillar misalignment and ultramicropores, are created during precursor manufacturing and subsequent heat treatment (Ref 28). The presence of these defects in carbon fibers resulted in the scattered tensile strength values. The presence of surface defects clearly affected the tensile strengths and Weibull moduli of the T1000GB fibers. The SEM results in Fig. 4 reveal that tensile failure in these fibers was initiated by surface defects. Surface modifications reduced the effects of the strength-limiting surface defects, which in turn improved the tensile strengths and Weibull moduli of the T1000GB fibers. In contrast, the failures of the K13D fibers were predominantly initiated by surface and internal defects. The SEM micrographs in Fig. 5 show that the gaps between crystallite sheets are the primary internal defect. Surface modifications also reduced the effects of the surface defects. In addition, the surface modifications covered the carbon fibers and the deformations in their radial directions, restraining the gaps (internal defects). The tensile strengths of the surface-modified K13D fibers improved because lower-strength fibers were removed from the sampling population when they broke, and the scatter of the tensile strength measurements decreased. Consequently, the surface modifications improved the average tensile strength and Weibull modulus of the K13D fibers.

3.4 Weibull Modulus Versus Tensile Strength

In a previous investigation (Ref 29, 30), we found that the Weibull modulus and the average tensile strength both increased as the gage length decreased for the as-received and CNT-grafted PAN- and pitch-based carbon fibers. Both types of fibers exhibited linear relationships between the Weibull modulus and the gage length and between the average tensile strength and the gage length on a log-log scale. Thus, the Weibull modulus and the average tensile strength are given by

$$m_f = \left(\frac{L}{L_0}\right)^{\alpha} \qquad \text{(Eq 6)}$$

and

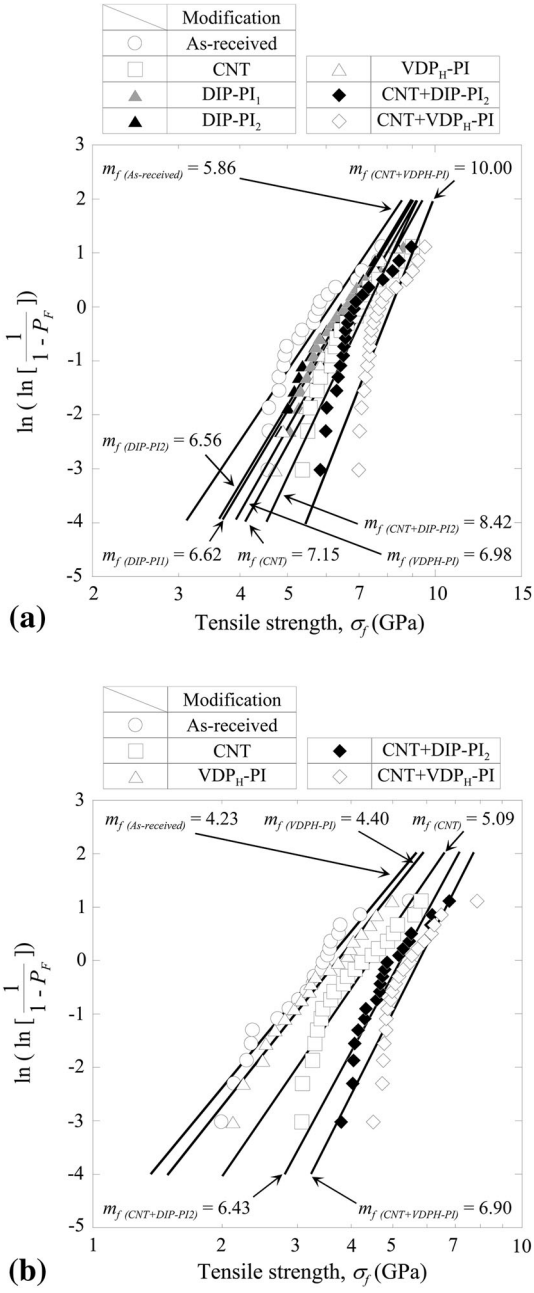

Fig. 6 Weibull plots for the as-received and surface-modified carbon fibers: *open square* CNT, *filled triangle* DIP-PI$_1$, *filled triangle* DIP-PI$_2$, *open triangle* VDP$_H$-PI, *filled diamond* CNT + DIP-PI$_2$, *open diamond* CNT + VDP$_H$-PI, and *open circle* as-received fibers. (a) T1000GB carbon fibers and (b) K13D carbon fibers

$$\sigma_{f.ave} = \sigma_0 \left(\frac{L_0}{L}\right)^{\frac{1}{m_f^*}}, \qquad \text{(Eq 7)}$$

respectively, where L_0, α, and m_f^* are the characteristic length, the length factor of the Weibull modulus, and the Weibull modulus obtained from the tensile strength versus gage length relationship, respectively.

From Eq 6 and 7, the Weibull modulus can be reformulated as

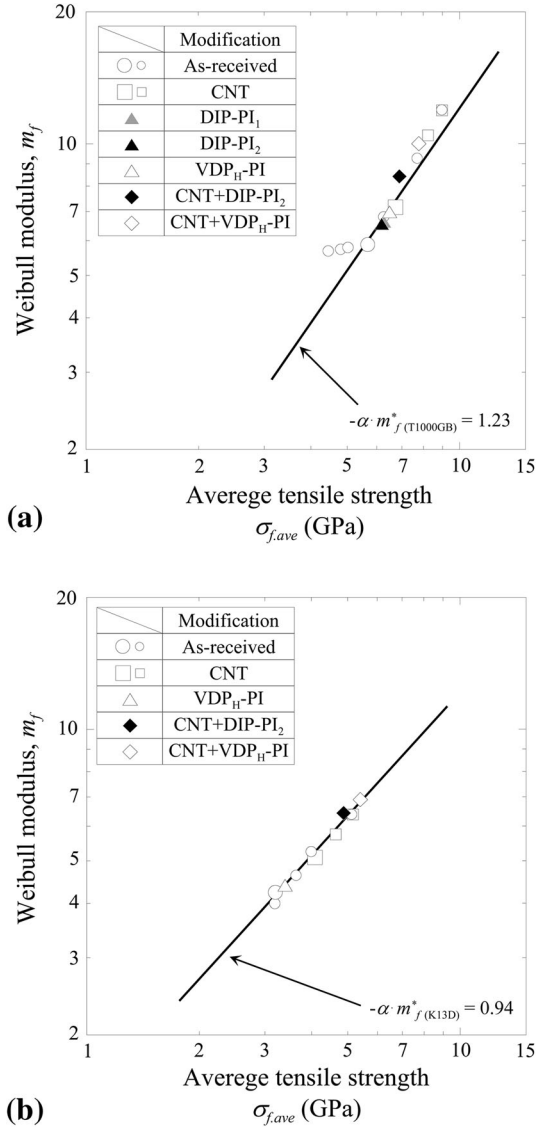

Fig. 7 Relationships between Weibull moduli and average tensile strengths of PAN- and pitch-based carbon fibers with different surface modifications: *open square* CNT, *filled triangle* DIP-PI$_1$, *filled triangle* DIP-PI$_2$, *open triangle* VDP$_H$-PI, *filled diamond* CNT + DIP-PI$_2$, *open diamond* CNT + VDP$_H$-PI, and ○-as-received fibers. (a) T1000GB carbon fibers and (b) K13D carbon fibers

$$m_f = \left(\frac{\sigma_{f.ave}}{\sigma_0}\right)^{-\alpha \cdot m_f^*}. \qquad \text{(Eq 8)}$$

Rearranging Eq 8 gives

$$\ln(m_f) = -\alpha \cdot m_f^* \ln(\sigma_{f.ave}) + \alpha \cdot m_f^* \ln(\sigma_0). \qquad \text{(Eq 9)}$$

Hence, a linear relationship between the Weibull modulus and the average tensile strength on a log-log scale can be obtained ("power law" relationship).

The relationships between Weibull modulus and average tensile strength are shown in Fig. 7 for surface-modified PAN- and pitch-based carbon fibers. The relationships between the Weibull moduli and the average tensile strengths of the as-received and CNT-grafted PAN- and pitch-based carbon fibers

were previously measured for several gage lengths (Ref 29, 30) and are also shown in Fig. 7. (The small square markers show the CNT-grafted carbon fibers at different gage lengths, and the small circular markers show the as-received carbon fibers at different gage lengths.) It is evident that there are linear relationships between the Weibull moduli and the average tensile strengths of the as-received and CNT-grafted PAN- and pitch-based carbon fibers on a log-log scale.[‡]

Surface modifications of the carbon fibers reduced the effects of the strength-limiting defects. In particular, the surface modifications corrected the surface flaws that were related to lower tensile strengths. This effect was similar to that of the gage lengths on the tensile strengths of the as-received carbon fibers. The fracture behaviors of the surface-modified carbon fibers were similar to those of the as-received carbon fibers at shorter gage lengths, which in turn improved the tensile strengths and Weibull moduli of the fibers.

4. Concluding Remarks

The tensile properties and Weibull statistical distributions of surface-modified PAN- and pitch-based single carbon fibers were measured. The results can be summarized as follows.

(1) For all surface modifications to the high-tensile-strength, PAN-based (T1000GB) carbon fibers and the high-tensile-modulus, pitch-based (K13D) carbon fibers, the stress was almost linearly proportional to the strain until failure. All surface modifications, especially the hybrid modifications (carbon nanotube grafting/PI coating), improved the tensile strengths of the T1000GB and K13D carbon fibers; the tensile moduli of all surface-modified carbon fibers were similar to those of the as-received fibers.
(2) The Weibull statistical distributions were examined for the surface-modified carbon fibers. All surface modifications, especially the hybrid surface modifications, improved the fibers' Weibull moduli.
(3) The Weibull modulus increased with the average tensile strength for the surface-modified carbon fibers. There were linear relationships between the Weibull moduli and the average tensile strengths of the carbon fibers on a log-log scale.

Acknowledgment

This work was supported by JSPS (Japan Society for the Promotion of Science) KAKENHI 26420715 and JST (Japan Science and Technology Agency) through Advanced Low Carbon Technology Research and Development Program (ALCA).

[‡]Several data points for the as-received carbon fibers did not fall on the line (T1000GB in Fig. 7(a)) when the gage length was >100 mm because the Weibull modulus stabilized at a larger value of the gage length than that at which the average tensile strength stabilized. The results clearly show that when the gage length was <100 mm, the Weibull moduli and the average tensile strengths of both the PAN- and pitch-based carbon fibers increased with decreasing gage length, and linear relationships were observed between the Weibull moduli and the average tensile strengths of the as-received and CNT-grafted carbon fibers on a log-log scale.

References

1. S. Chand, Review-Carbon Fibers for Composites, *J. Mater. Sci.*, 2000, **35**(6), p 1303–1313
2. K. Naito, Y. Tanaka, J.M. Yang, and Y. Kagawa, Tensile Properties of Ultrahigh Strength PAN-Based, Ultrahigh Modulus Pitch-Based and High Ductility Pitch-Based Carbon Fibers, *Carbon*, 2008, **46**(2), p 189–195
3. K. Naito, Y. Tanaka, J.M. Yang, and Y. Kagawa, Flexural Properties of PAN- and Pitch-Based Carbon Fibers, *J. Am. Ceram. Soc.*, 2009, **92**(1), p 186–192
4. T.D. Juska and P.M. Puckett, Matrix Resins and Fiber/Matrix Adhesion, *Composites Engineering Handbook*, P.K. Mallick, Ed., New York, Dekker, 1997, p 101–165
5. W.B. Downs and R.T.K. Baker, Novel Carbon Fiber-Carbon Filament Structures, *Carbon*, 1991, **29**(8), p 1173–1179
6. S. Zhu, C.H. Su, S.L. Lehoczky, I. Muntele, and D. Ila, Carbon Nanotube Growth on Carbon Fibers, *Diam. Relat. Mater.*, 2003, **12**(10–11), p 1825–1828
7. J.O. Zhao, L. Liu, Q.G. Guo, J.L. Shi, G.T. Zhai, J.R. Song, and Z.J. Liu, Growth of Carbon Nanotubes on the Surface of Carbon Fibers, *Carbon*, 2008, **46**(2), p 380–383
8. K. Naito, J.M. Yang, Y. Tanaka, and Y. Kagawa, Tensile Properties of Carbon Nanotubes Grown on Ultrahigh Strength Polyacrylonitrile-Based and Ultrahigh Modulus Pitch-Based Carbon Fibers, *Appl. Phys. Lett.*, 2008, **92**(23), p 231912-1-3
9. K. Naito, J.M. Yang, Y. Xu, and Y. Kagawa, Enhancing the Thermal Conductivity of Polyacrylonitrile- and Pitch-Based Carbon Fibers by Grafting Carbon Nanotubes on Them, *Carbon*, 2010, **48**(6), p 1849–1857
10. J.K. Kim and Y.W. Mai, Effects of Interfacial Coating and Temperature on the Fracture Behaviors of Unidirectional Kevlar and Carbon-Fiber Reinforced Epoxy-Resin Composites, *J. Mater. Sci.*, 1991, **26**(17), p 4702–4720
11. P.C. Varelidis, R.L. McCullough, and C.D. Papaspyrides, The Effect on the Mechanical Properties of Carbon/Epoxy Composites of Polyamide Coatings on the Fibers, *Compos. Sci. Technol.*, 1999, **59**(12), p 1813–1823
12. S. Dujardin, R. Lazzaroni, L. Rigo, J. Riga, and J.J. Verbist, Electrochemically Polymer-Coated Carbon-Fibers—Characterization and Potential for Composite Applications, *J. Mater. Sci.*, 1986, **21**(12), p 4342–4346
13. B. Zinger, S. Shkolnik, and H. Höcke, Electrocoating of Carbon-Fibers with Polyaniline and Poly(hydroxyalkyl methacrylates), *Polymer*, 1989, **30**(4), p 628–635
14. L.T. Drzal, Adhesion of Graphite Fibers to Epoxy Matrices 2. The Effect of Fiber Finish, *J. Adhes.*, 1983, **16**(2), p 133–152
15. R.J. Dauksys, Graphite Fiber Treatments Which Affect Fiber Surface Morphology and Epoxy Bonding Characteristics, *J. Adhes.*, 1973, **5**(3), p 211–244
16. T. Naganuma, K. Naito, and J.M. Yang, High-Temperature Vapor Deposition Polymerization Polyimide Coating for Elimination of Surface Nano-Flaws in High-Strength Carbon Fiber, *Carbon*, 2011, **49**(12), p 3881–3890
17. K. Naito, The Effect of High-Temperature Vapor Deposition Polymerization of Polyimide Coating on Tensile Properties of Polyacrylonitrile- and Pitch-Based Carbon Fibers, *J. Mater. Sci.*, 2013, **48**(17), p 6056–6064
18. A.R. Bunsell and B. Harris, Hybrid Carbon and Glass Fibre Composites, *Composites*, 1974, **5**(4), p 157–164
19. K.M. Hardaker and M.O.W. Richardson, Trends in Hybrid Composite Technology, *Polym.-Plast. Technol.*, 1980, **15**(2), p 169–182
20. K. Naito, J.M. Yang, and Y. Kagawa, Tensile Properties of High Strength Polyacrylonitrile (PAN)-Based and High Modulus Pitch-Based Hybrid Carbon Fibers-Reinforced Epoxy Matrix Composite, *J. Mater. Sci.*, 2012, **47**(6), p 2743–2751
21. K. Naito, Tensile Properties of Polyacrylonitrile- and Pitch-Based Hybrid Carbon Fiber/Polyimide Composites with Some Nanoparticles in the Matrix, *J. Mater. Sci.*, 2013, **48**(12), p 4163–4176
22. T. Naganuma, K. Naito, J.M. Yang, J. Kyono, D. Sasakura, and Y. Kagawa, The Effect of a Compliant Polyimide Nanocoating on the Tensile Properties of a High Strength PAN-Based Carbon Fiber, *Compos. Sci. Technol.*, 2009, **69**(7–8), p 1319–1322
23. A. Kubono, H. Higuchi, S. Umemoto, and N. Okui, Direct Formation of Polyimide Thin Films by Vapor Deposition Polymerization, *Thin Solid Films*, 1993, **232**(2), p 256–260

24. H. Hatori, Y. Yamada, M. Shiraishi, and Y. Takahashi, Carbonization and Graphitization of Polyimide Coating on Carbon-Fiber, *Carbon*, 1991, **29**(4–5), p 679–680
25. American Society for Testing and Materials, Standard Test Method for Tensile Strength and Young's Modulus of Fibers, in ASTM C1557-03, *ASTM Annual Book of Standards, Vol. 15.01. 2013*, American Society for Testing and Materials, West Conshohocken, PA, 2013
26. M.G. Sung, K. Sassa, T. Tagawa, T. Miyata, H. Ogawa, M. Doyama, S. Yamada, and S. Asai, Application of a High Magnetic Field in the Carbonization Process to Increase the Strength of Carbon Fibers, *Carbon*, 2002, **40**(11), p 2013–2020
27. W. Weibull, A Statistical Distribution Function of Wide Applicability, *J. Appl. Mech.*, 1951, **18**, p 293–297
28. W. Johnson, *The Structure of PAN Based Carbon Fibres and Relationship to Physical Properties*, *Strong Fibers*, W. Watt and B.V. Perov, Eds., vol 1, Amsterdam, Elsevier, 1985, p 389–443
29. K. Naito, J.M. Yang, Y. Tanaka, and Y. Kagawa, The Effect of Gauge Length on Tensile Strength and Weibull Modulus of Polyacrylonitrile (PAN)- and Pitch-Based Carbon Fibers, *J. Mater. Sci.*, 2012, **47**(2), p 632–642
30. K. Naito, J.M. Yang, Y. Inoue, and H. Fukuda, The Effect of Surface Modification with Carbon Nanotubes Upon the Tensile Strength and Weibull Modulus of Carbon Fibers, *J. Mater. Sci.*, 2012, **47**(23), p 8044–8051